Physical characterization of latent tuberculosis lesions from post-mortem human lung tissue

Delon Naicker[1], Gordon Wells[1], Kapongo Lumamba[1], Kievershen Nargan[1], Threnesan Naidoo[1,4] Adrie JC Steyn[1, 2, 3*]

[1] *Africa Health Research Institute, University of KwaZulu-Natal, Durban, South Africa.*
[2] *Department of Microbiology, University of Alabama at Birmingham, Birmingham, AL, USA.*
[3] *Centers for AIDS Research and Free Radical Biology, University of Alabama at Birmingham, Birmingham, AL, USA.*
[4] *Department of Medicine & Pathology, Waler Sisulu University, Mthatha, South Africa.*
*Corresponding author

Background

Approximately one-third of the global population is thought to be infected with tuberculosis (TB). A latent tuberculosis infection (LTBI) is characterized by a permanent immune response to *Mycobacterium tuberculosis* (*Mtb*) antigens in the absence of any clinical manifestation of the disease. During an LTBI, *Mtb* remains in an inactive state for a long time, being phenotypically insusceptible to anti-tuberculous drugs and retaining its ability to resuscitate and proliferate. Several historical studies have shown that calcified lesions were identified in latent TB post-mortem (PM) specimens.

High-resolution digital 3D imaging of TB lesions within human post-mortem lung tissue will improve our understanding of TB disease. X-ray computed tomography (CT) is an invaluable tool for non-destructive imaging in medical diagnosis. Compared to medical CT, nano/micro-CT (n/µCT) uses higher energy X-rays and smaller rotations between the sample and detector (< 1°) to generate much higher resolution.

Study rationale

Our current understanding of TB is limited by conventional histological methods based on the 2D assessment of small regions of interest. This requires the need for high-resolution three-dimensional (3D) imaging techniques to visualize TB lesions within the context of the whole lung.

Study objective

Given the availability of PM human lung tissue and advancements in 3D imaging techniques, the objective of this study is to utilize VGStudio Max to determine the physical characteristics and spatial distribution of TB lesions in PM tissue from decedents that died of causes other than TB.

Methods and materials

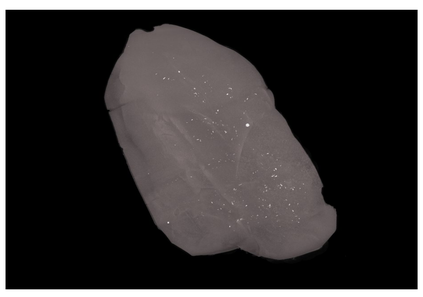

Complete reconstructed µ/CT scanned images of the lungs were used for the analysis.

Subsequent visualization and analysis (*e.g.*, dimensions, surface area, volume calculations etc) were performed in Volume Graphics VGStudio Max.

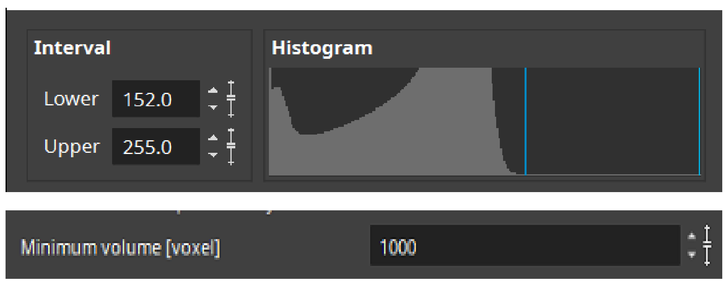

Grey-scale thresholding was employed for segmentation (demarcation of 3D regions of interest) and a minimum voxel size of 1000 voxels was maintained for all the samples to establish consistency.

Results

Table 1: The physical parameters for post-mortem 1.

Lesion Number	Total Volume	Surface Area	Dimensions		
	mm^3	mm^2	mm	mm	mm
Lesion 1	1.48	8.33	2.07	1.67	1.58
Lesion 2	0.35	3.36	1.17	0.86	1.89
Lesion 3	0.30	2.51	0.81	0.77	1.13
Lesion 4	0.28	2.33	0.99	0.81	0.86
Lesion 5	0.26	2.23	0.95	0.77	0.90
Lesion 6	0.19	1.92	0.68	0.77	1.08
Lesion 7	0.17	2.09	0.72	0.50	1.35
Lesion 8	0.12	1.41	0.68	0.77	0.68
Lesion 9	0.12	1.21	0.63	0.54	0.63
Lesion 10	0.11	1.20	0.72	0.50	0.59

The ten largest calcified lesions based on volume were identified. Further, the largest calcified lesion detected had dimensions of 2.07 mm x 1.67 mm x 1.58 mm, a volume of 1.48 mm^3, and a surface area of 8.33 mm^2. The smallest calcified lesion had dimensions of 0.72 mm x 0.50 mm x 0.59 mm, a volume of 0.11 mm^3, and a surface area of 1.20 mm^2.

Figure 1: The spatial distribution of the ten largest lesions based on volume identified in post-mortem 1.

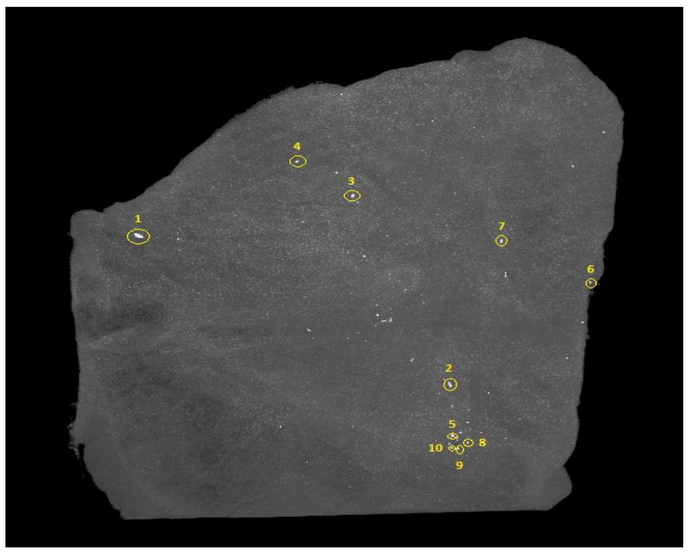

Table 2: The physical parameters for post-mortem 2.

Lesion Number	Total Volume	Surface Area	Dimensions		
	mm^3	mm^2	mm	mm	mm
Lesion 1	4.98	18.85	2.30	2.75	2.39
Lesion 2	0.94	5.50	1.85	1.08	1.26
Lesion 3	0.85	5.21	1.53	1.31	1.13
Lesion 4	0.43	3.48	1.08	1.04	1.40
Lesion 5	0.27	2.89	1.35	0.68	1.22
Lesion 6	0.23	2.34	1.26	1.04	0.68
Lesion 7	0.17	1.93	0.99	1.04	0.59
Lesion 8	0.15	1.97	0.86	1.44	0.68
Lesion 9	0.10	1.25	0.68	0.41	0.81
Lesion 10	0.09	1.11	0.72	0.50	0.59

The ten largest calcified lesions based on volume were identified. Further, the largest calcified lesion detected had dimensions of 2.30 mm x 2.75 mm x 2.39 mm, a volume of 4.98 mm^3, and a surface area of 18.85 mm^2. The smallest calcified lesion had dimensions of 0.72 mm x 0.50 mm x 0.59 mm, a volume of 0.09 mm^3, and a surface area of 1.11 mm^2.

Figure 2: The spatial distribution of the ten largest lesions based on volume identified in post-mortem 2.

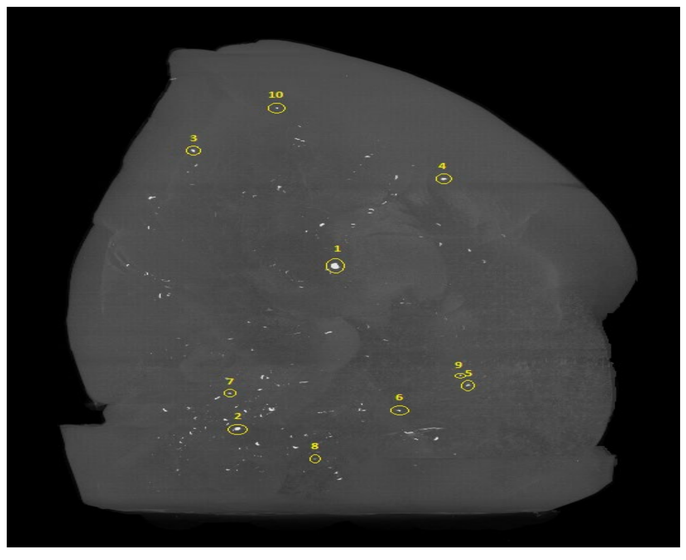

Table 3: The physical parameters for post-mortem 3.

Lesion Number	Total Volume	Surface Area	Dimensions		
	mm^3	mm^2	mm	mm	mm
Lesion 1	1.52	8.48	1.53	1.71	1.85
Lesion 2	0.96	6.29	1.76	1.49	1.26
Lesion 3	0.38	2.79	0.99	0.99	0.86
Lesion 4	0.36	2.75	0.77	0.99	1.13
Lesion 5	0.23	2.19	0.90	0.90	0.86
Lesion 6	0.21	2.40	0.77	0.99	1.17
Lesion 7	0.21	1.91	0.81	0.77	0.77
Lesion 8	0.14	1.47	0.63	0.63	0.63
Lesion 9	0.12	1.27	0.54	0.72	0.72
Lesion 10	0.09	1.27	0.50	0.63	0.81

The ten largest calcified lesions based on volume were identified. Further, the largest calcified lesion detected had dimensions of 1.53 mm x 1.71 mm x 1.85 mm, a volume of 1.52 mm^3, and a surface area of 8.48 mm^2. The smallest calcified lesion had dimensions of 0.50 mm x 0.63 mm x 0.81 mm, a volume of 0.09 mm^3, and a surface area of 1.27 mm^2.

Figure 3: The spatial distribution of the ten largest lesions based on volume identified in post-mortem 3.

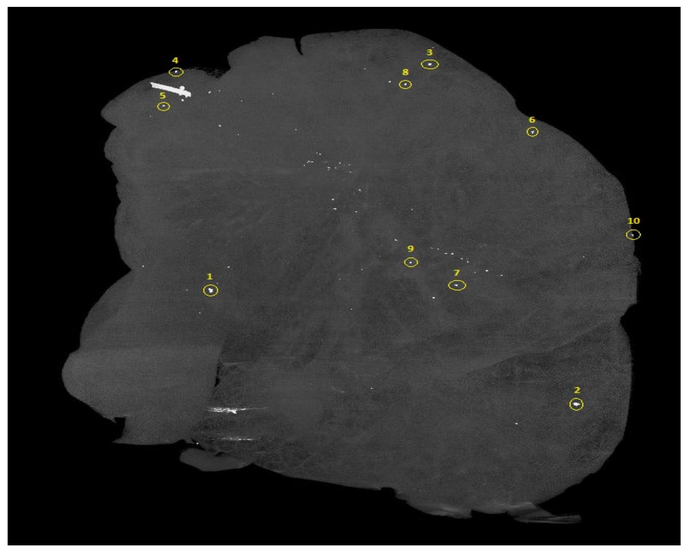

Conclusion

The results of this study suggest that µCT is a powerful imaging tool while VGStudio Max presents a useful platform to determine the physical characteristics of calcified TB lesions in PM tissue. Future work would require segmenting each calcified lesion of interest to determine its 3D structure.

Acknowledgements

This work was supported by NIH grants R01AI111940, R01AI134810, R01AI137043, R33AI138280, and R21A127182, Bill and Melinda Gates Foundation award OPP1130017, funding from the Wellcome Leap ΔTissue Program, and pilot funds from the UAB CFAR and UAB Heersink School of Medicine to AJCS. Additional support came from CRDF Global, the South African Medical Research Council, and a South African NRF BRICS Multilateral grant to AJCS. Other support included R35HL135816-04S1, P30DK072482, and U01HL152978 to SMR; 5F31HL146083-02 and 2T32HL105346-11A1 to JEPL and 3T32GM008361-30S1 to HP and JEPL. This work was also supported by the Cystic Fibrosis Foundation (ROWE19R0) to SMR, and a Bill and Melinda Gates Foundation Award OPP1116944 to AS.